

Scientific paper

Study of the Crystallization Fields of Vanadyl(IV) Selenites in the System $\text{VOSeO}_3 - \text{SeO}_2 - \text{H}_2\text{O}$

Velyana Georgieva,¹ Mariana Tavlieva,¹ Lyubomir Vlaev^{1,*}
and Svetlana Genieva²

¹ Department of Physical Chemistry, Assen Zlatarov University, 8010 Burgas, Bulgaria,

² Department of Inorganic and Analytical Chemistry, Assen Zlatarov University, 8010 Burgas

* Corresponding author: E-mail: vlaev@btu.bg

Phone: +359 56 858 346, Fax: +359 56 880 249

Received: 16-03-2012

Abstract

The solubility of $\text{VOSeO}_3 - \text{SeO}_2 - \text{H}_2\text{O}$ system was studied within the temperature interval 50–300 °C. The phase diagram of vanadyl(IV) selenites was plotted and the crystallization fields were determined for the different phases. Depending on the conditions for hydrothermal synthesis, several types of selenites were obtained – $[\text{VO}(\text{SeO}_3)(\text{H}_2\text{O})_2] \cdot 0.5 \text{H}_2\text{O}$, $\text{VOSeO}_3 \cdot \text{H}_2\text{O}$, VOSeO_3 and VOSe_2O_5 . The different phases were established and characterized by chemical, thermal and powder X-ray diffraction analyses, as well as by IR spectroscopy.

Keywords: Vanadyl(IV) selenites, hydrothermal synthesis, IR spectroscopy, X-ray diffraction, solubility diagrams

1. Introduction

Vanadium forms a great number of compounds due to its variable oxidation states (II, III, IV and V), participating in the cation or anion part. In literature various inorganic vanadium and organovanadium selenium-containing compounds are described,^{1–10} which are intensively studied in recent years because of their possible usage as mighty anti-diabetic drugs and anticancer agents.^{11,12} Some vanadyl(IV) selenites have magnetic properties and they are potentially useful for new sensors.^{13,14} Vanadium(IV) phosphates have been intensively studied due to their catalytic and electrochemical applications¹⁵ and they are considered as potential lithium battery electrodes.¹⁶ In selenium compounds SeO_3^{2-} ions have structural similarity with PO_4^{3-} ions,¹⁷ which suggests that vanadyl(IV) selenites could be used as electrode in lithium batteries, for catalytic or electrochemical applications.

The following vanadium(IV) oxo selenites have been synthesized: $\text{VOSeO}_3 \cdot 3\text{H}_2\text{O}$, $[\text{VO}(\text{SeO}_3)(\text{H}_2\text{O})_2] \cdot 0.5\text{H}_2\text{O}$, $\text{VOSeO}_3 \cdot \text{H}_2\text{O}$, VOSeO_3 , VOSe_2O_5 and $\text{VO}(\text{SeO}_2\text{OH})_2$.^{13,15,18–22} There have also been reported bimetallic vanadyl(IV) selenites: $\text{K}(\text{VO})(\text{SeO}_3)_2$, $\text{Cu}(\text{VO})(\text{SeO}_3)_2$ and $\text{Ba}(\text{VO})_2(\text{SeO}_3)_2(\text{HSeO}_3)_2$.^{17,23,24}

The lack of systematic approach in most of the studies cited does not allow to determine clearly the types and the number of the different solid phases which are in equilibrium with the liquid phase at various temperatures, as well as the boundaries of the crystallization fields of the known vanadyl(IV) selenites in the system $\text{VOSeO}_3 - \text{SeO}_2 - \text{H}_2\text{O}$. In this respect, some useful information can be obtained from the dissolution isotherms of the system at different temperatures and the values of the parameters characterizing the non-variant (peritonic) points, namely the number of phases and crystallization fields at a certain temperature.

The focus of the present study is to define the crystallization fields in the system $\text{VOSeO}_3 - \text{SeO}_2 - \text{H}_2\text{O}$ within the temperature interval 50–300 °C and to characterize the observed phases.

2. Experimental

2.1. Synthesis

The initial substance used for the synthesis of the subsequent selenites, was $\text{VOSeO}_3 \cdot \text{H}_2\text{O}$. It was prepared by precipitation of a 0.6 mol dm^{-3} aqueous solution of vanadium(IV) oxide sulphate hydrate puriss (Riedel-de

Hañen) with a 0.6 mol dm^{-3} aqueous solution of sodium selenite pentahydrate puriss (Fluka) at $25 \text{ }^\circ\text{C}$. The solutions with volumes of 1 dm^3 were slowly mixed ($5 \text{ cm}^3 \text{ min}^{-1}$) under continuous stirring with a blade mixer. The obtained precipitate was left to “age” in the initial solution at room temperature for a week. The formed crystalline substance was collected on a G4 frit, rinsed vigorously with deionized distilled water and dried in air at ambient temperature for another week. The isolated compound was light green fine powder, which was stable in air at laboratory temperature. The results from the chemical and powder X-ray analyses showed the compound had net formula $\text{VOSeO}_3 \cdot \text{H}_2\text{O}$. 20 cm^3 teflon-lined steel vessels were used for the experiment. $1 \text{ g VOSeO}_3 \cdot \text{H}_2\text{O}$ and 10 cm^3 aqueous solution of SeO_2 purum (Aldrich) with concentrations varying from 5 to 70 mass % SeO_2 were placed in these vessels at 5% steps. The time required for equilibration of the individual samples was from 3 months (at $50 \text{ }^\circ\text{C}$) to 10 days (at $300 \text{ }^\circ\text{C}$). The temperatures of the hydrothermal synthesis ranged from 50 to $300 \text{ }^\circ\text{C}$ in $50 \text{ }^\circ\text{C}$ intervals. At the end of the experiment, the vessels were cooled and opened and the precipitate was filtered through porous glass filter. Both the precipitate and the filtrate were analyzed to determine the contents of vanadium(IV) and selenium(IV). Vanadium(IV) and selenium(IV) were determined, applying a combined oxidation–reduction titrimetric methods.²⁵ The *Schreinemaker's* method was used to study the solubility in the $\text{VOSeO}_3 - \text{SeO}_2 - \text{H}_2\text{O}$ system. The solubility diagram was plotted according to *Gibbs–Roozeboom* method. The approach and characterization method for solid phases were similar to the described in the literature.^{26–29}

2. 2. X-ray Powder Diffraction

Powder X-ray patterns were taken on a wide angle X-ray diffractometer with a goniometer URD–6 (Ger-

many), using cells with a diameter of 12 mm, CoK_α radiation ($\lambda = 1.78892 \text{ \AA}$) and an iron filter for β -emission. The lattice parameters were derived from 150–165 accurately measured reflections in the range $3 \leq 2\theta \leq 60$. The structures were solved by Patterson or direct methods and refined with the least squares method.

2. 3. Thermal Analysis

The thermal decomposition of the samples was performed on a F. Paulik–I. Paulik–L. Erdely apparatus (MOM, Hungary) by heating to $800 \text{ }^\circ\text{C}$ at heating rate 5 and $10 \text{ }^\circ\text{C min}^{-1}$ in static air. The samples (50 or 100 mg) were vigorously ground in an agate vibration mortar and placed in a platinum crucible (7 mm diameter and 14 mm height). The standard used was $\alpha\text{-Al}_2\text{O}_3$ heated to $1100 \text{ }^\circ\text{C}$. The curves were registered with resolutions $1/5$ for DTA, $1/15$ for DTG and 1 mg for TG.

2. 4. Vibrational Spectroscopy

The IR absorption spectra were taken on a spectrophotometer Specord-75 (Carl Zeiss, Jena, Germany) over the region from 400 to 4000 cm^{-1} (resolution 2 cm^{-1}). The experiments were carried out at room temperature using KBr pellets with concentration of the studied substance $0.3 \text{ mass}\%$.

3. Results and Discussion

The content of V(IV) and Se(IV) was determined in the equilibrium liquid phases as well as in the wet solid phases obtained at the hydrothermal synthesis.²⁵ Table 1 illustrates the experimental results for the phases, obtained at $50 \text{ }^\circ\text{C}$.

Table 1. Composition of liquid and solid phases in solubility isotherm of the system $\text{VOSeO}_3 - \text{SeO}_2 - \text{H}_2\text{O}$ at $50 \text{ }^\circ\text{C}$.

Liquid phase (mass %)			Solid phase (mass %)			Formula composition of solid phase
VOSeO_3	SeO_2	H_2O	VOSeO_3	SeO_2	H_2O	
2.18	5.91	91.91	59.23	1.38	39.38	$[\text{VO}(\text{SeO}_3)(\text{H}_2\text{O})_2] \cdot 0.5\text{H}_2\text{O}$
4.40	12.40	83.20	60.41	2.79	36.79	$[\text{VO}(\text{SeO}_3)(\text{H}_2\text{O})_2] \cdot 0.5\text{H}_2\text{O}$
4.74	17.43	77.83	60.60	3.90	35.50	$[\text{VO}(\text{SeO}_3)(\text{H}_2\text{O})_2] \cdot 0.5\text{H}_2\text{O}$
5.40	21.90	72.70	61.37	4.51	34.11	$[\text{VO}(\text{SeO}_3)(\text{H}_2\text{O})_2] \cdot 0.5\text{H}_2\text{O}$
5.60	27.00	67.40	60.87	5.87	33.27	$[\text{VO}(\text{SeO}_3)(\text{H}_2\text{O})_2] \cdot 0.5\text{H}_2\text{O}$
6.25	33.13	60.63	60.27	7.46	32.26	$[\text{VO}(\text{SeO}_3)(\text{H}_2\text{O})_2] \cdot 0.5\text{H}_2\text{O}$
6.31	37.34	56.34	59.03	9.79	31.19	$[\text{VO}(\text{SeO}_3)(\text{H}_2\text{O})_2] \cdot 0.5\text{H}_2\text{O}$
6.31	37.34	56.34	68.97	7.52	23.52	$[\text{VO}(\text{SeO}_3)(\text{H}_2\text{O})_2] \cdot 0.5\text{H}_2\text{O}$ and $\text{VOSeO}_3 \cdot \text{H}_2\text{O}$
6.31	37.34	56.34	76.07	8.06	15.86	$\text{VOSeO}_3 \cdot \text{H}_2\text{O}$
6.20	42.90	50.90	76.80	8.90	14.30	$\text{VOSeO}_3 \cdot \text{H}_2\text{O}$
5.70	47.20	47.10	78.21	9.00	12.80	$\text{VOSeO}_3 \cdot \text{H}_2\text{O}$
4.80	54.80	40.40	77.67	10.67	11.67	$\text{VOSeO}_3 \cdot \text{H}_2\text{O}$
4.63	59.58	35.78	76.12	12.64	11.24	$\text{VOSeO}_3 \cdot \text{H}_2\text{O}$
2.50	68.60	28.90	77.06	13.47	9.47	$\text{VOSeO}_3 \cdot \text{H}_2\text{O}$

As can be seen from Table 1, the solubility of $[\text{VO}(\text{SeO}_3)(\text{H}_2\text{O})_2] \cdot 0.5\text{H}_2\text{O}$ increased with the increase of SeO_2 concentrations in the range from 5.91 to 37.34 mass%. The composition in the peritonic point was: 6.31 mass% VOSeO_3 , 37.34 mass% SeO_2 and 56.34 mass% H_2O . With the increase of SeO_2 concentration from 37.34 to 68.60 mass% the solubility of $\text{VOSeO}_3 \cdot \text{H}_2\text{O}$ decreased to 2.50 mass% VOSeO_3 , 68.60 mass% SeO_2 and 28.90 mass% H_2O .

The data from the chemical analysis were used for plotting six solubility isotherms of the system applying the *Schreinemaker's* method for each of the studied temperatures – 50, 100, 150, 200, 250 and 300 °C. Figure 1 presents the solubility isotherms at 50 °C and 250 °C.

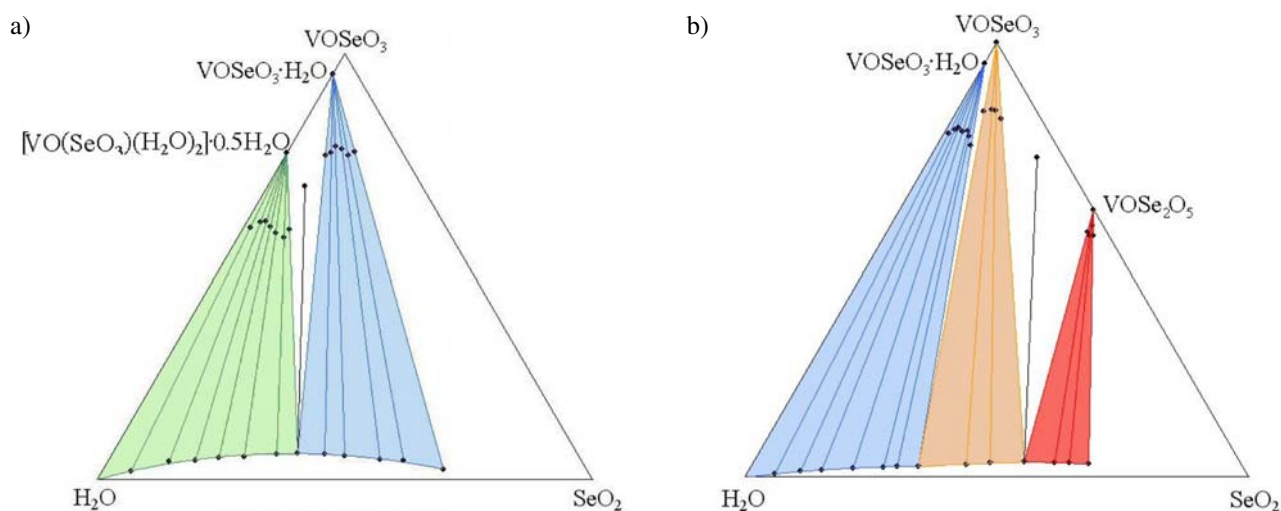


Figure 1. Solubility isotherms of the system $\text{VOSeO}_3 - \text{SeO}_2 - \text{H}_2\text{O}$: **A**– at 50 °C; **B**– at 250 °C.

Figure 1A shows the formation of two crystallization fields, corresponding to the phases of $[\text{VO}(\text{SeO}_3)(\text{H}_2\text{O})_2] \cdot 0.5\text{H}_2\text{O}$ and $\text{VOSeO}_3 \cdot \text{H}_2\text{O}$, while Figure 1B shows three crystallization fields, corresponding to $\text{VOSeO}_3 \cdot \text{H}_2\text{O}$, VOSeO_3 and VOSe_2O_5 . On the

basis of the chemical analysis data and the solubility isotherms for each temperature the number of peritonic points and their composition were determined in the system, as well as the type of solid phases, which were in equilibrium at the respective temperatures (Table 2).

The experimental results revealed that in the system $\text{VOSeO}_3 - \text{SeO}_2 - \text{H}_2\text{O}$ four solid phases could be distinguished depending on the hydrothermal synthesis temperature – $[\text{VO}(\text{SeO}_3)(\text{H}_2\text{O})_2] \cdot 0.5\text{H}_2\text{O}$, $\text{VOSeO}_3 \cdot \text{H}_2\text{O}$, VOSeO_3 and VOSe_2O_5 . One peritonic point could be observed at temperatures lower than 150 °C and above this threshold there are two such points. The solid phases were characterized using chemical and powder X-ray diffraction analysis and IR spectroscopy. Table 3 presents the inter-planar distance d [Å] and the relative intensities I [%]

of the most intensive lines of the pure solid phases of $[\text{VO}(\text{SeO}_3)(\text{H}_2\text{O})_2] \cdot 0.5\text{H}_2\text{O}$, $\text{VOSeO}_3 \cdot \text{H}_2\text{O}$, VOSeO_3 and VOSe_2O_5 .

The parameters of the elementary cell were determined for each of the four vanadyl(IV) selenites. Our results

Table 2. Equilibrium solid phases and composition at the peritonic points of the isotherms of the ternary system $\text{VOSeO}_3 - \text{SeO}_2 - \text{H}_2\text{O}$ in the temperature range 50–300 °C and the corresponding composition of the liquid phase in mass%.

T (°C)	Component [mass%]			Equilibrium solid phases at the peritonic points	
	VOSeO_3	SeO_2	H_2O	Phase 1	Phase 2
50	6.31	37.3	56.3	$[\text{VO}(\text{SeO}_3)(\text{H}_2\text{O})_2] \cdot 0.5\text{H}_2\text{O}$	$\text{VOSeO}_3 \cdot \text{H}_2\text{O}$
100	2.88	27.8	69.3	$[\text{VO}(\text{SeO}_3)(\text{H}_2\text{O})_2] \cdot 0.5\text{H}_2\text{O}$	$\text{VOSeO}_3 \cdot \text{H}_2\text{O}$
150	4.37	15.8	79.8	$[\text{VO}(\text{SeO}_3)(\text{H}_2\text{O})_2] \cdot 0.5\text{H}_2\text{O}$	$\text{VOSeO}_3 \cdot \text{H}_2\text{O}$
200	1.01	6.29	92.7	$[\text{VO}(\text{SeO}_3)(\text{H}_2\text{O})_2] \cdot 0.5\text{H}_2\text{O}$	$\text{VOSeO}_3 \cdot \text{H}_2\text{O}$
200	4.10	53.7	42.3	$\text{VOSeO}_3 \cdot \text{H}_2\text{O}$	VOSeO_3
250	2.54	33.2	64.2	$\text{VOSeO}_3 \cdot \text{H}_2\text{O}$	VOSeO_3
250	3.52	53.7	42.7	VOSeO_3	VOSe_2O_5
300	3.40	13.3	83.3	$\text{VOSeO}_3 \cdot \text{H}_2\text{O}$	VOSeO_3
300	3.53	30.0	66.4	VOSeO_3	VOSe_2O_5

Table 3. Interplanar distance (Å) and relative intensity (%) of the peaks.

[VO(SeO ₃)(H ₂ O) ₂] · 0.5H ₂ O			VOSeO ₃ · H ₂ O			VOSeO ₃			VOSe ₂ O ₅		
<i>d</i> (Å)	<i>I</i> (%)	<i>h k l</i>	<i>d</i> (Å)	<i>I</i> (%)	<i>h k l</i>	<i>d</i> (Å)	<i>I</i> (%)	<i>h k l</i>	<i>d</i> (Å)	<i>I</i> (%)	<i>h k l</i>
5.2581	99	2 0 -2	6.2592	22	0 0 1	4.8910	8	0 2 0	5.1224	27	2 1 0
4.6832	4	1 1 1	5.1517	3	1 -1 0	4.1764	6	0 2 1	4.2682	26	2 1 1
4.1619	4	3 1 0	4.4535	10	0 1 -1	3.9539	100	1 0 0	3.9647	25	2 2 0
3.4239	3	3 1 1	3.8369	100	0 1 1	3.6741	36	1 1 0	3.7640	30	3 0 0
3.0457	61	3 1 -3	3.1127	21	0 0 2	3.5203	10	1 1 -1	3.6026	44	3 1 0
2.9805	5	0 2 1	2.8606	10	2 -1 -1	3.1346	7	1 1 1	3.4847	100	1 1 2
2.7685	9	5 1 -3	2.5477	21	1 1 1	3.0777	34	1 2 0	3.2905	23	3 1 1
2.7025	8	2 2 -2	2.4586	13	2 -1 1	3.0142	20	0 3 1	3.1319	79	3 2 0
2.5655	25	5 1 1	2.3710	13	0 2 1	2.9216	10	1 1 -2	3.0974	22	2 1 2
2.5159	4	4 2 0	2.2065	6	0 2 -2	2.5988	16	1 2 -2	2.8980	42	3 2 1
2.4626	24	7 1 -2	2.0856	10	2 -2 -2	2.5117	15	0 3 2	2.8105	41	4 0 0
2.3657	7	0 0 4	2.0360	9	2 1 -1	2.3457	11	0 4 1	2.7884	31	2 2 2
2.2807	5	4 2 1	1.9988	6	1 -1 -3	2.0513	17	0 3 3	2.3435	72	2 1 3
2.2287	3	0 2 3	1.9580	3	3 -1 -1	2.0035	8	1 1 3	2.1556	23	4 3 1
2.1343	5	7 1 -4	1.9169	6	3 -2 -1	1.9660	10	1 4 1	2.0360	37	5 2 1
2.1035	4	8 0 -4	1.9048	31	2 -3 -1	1.9441	9	2 1 0	1.9962	23	3 2 3
2.0856	17	1 1 4	1.8779	4	2 -2 2	1.9095	11	1 4 -2	1.9879	22	4 4 0
1.9787	11	9 1 -2	1.8152	5	3 -1 -2	1.9001	16	0 5 1	1.9630	22	0 0 4
1.9575	4	9 1 -3	1.7713	3	3 -2 -2	1.8617	7	1 1 -4	1.9358	23	1 0 4
1.9276	5	3 3 -2	1.7512	3	1 -3 2	1.8340	15	2 2 0	1.9057	19	1 1 4
1.8903	5	0 2 4	1.7466	3	3 -2 1	1.7920	8	0 4 3	1.8903	20	4 1 3
1.8698	41	10 0 -2	1.7297	4	1 -2 3	1.7733	8	2 2 -2	1.7994	20	6 1 1
1.8662	37	1 3 2	1.7053	4	3 -3 0	1.7614	10	1 2 -4	1.7598	16	2 2 4
1.8186	4	3 1 4	1.6873	4	1 -2 -3	1.7327	7	2 2 1	1.7500	17	5 4 0
1.7646	3	7 1 2	1.6724	4	0 3 -2	1.7047	7	2 3 -1	1.7346	19	6 2 1
1.7380	7	5 3 -3	1.6489	4	2 -3 2	1.6844	7	1 5 1	1.7251	19	5 3 2
1.6945	100	2 0 -6	1.6547	4	1 -3 -2	1.6626	8	2 0 2	1.6752	20	6 3 0
1.6547	3	7 1 -6	1.6271	3	1 2 -3	1.6404	10	2 1 2	1.6163	23	6 2 2
1.5732	4	5 3 0	1.5993	4	1 0 -4	1.6225	7	2 2 -3	1.6057	36	7 0 0
1.5513	4	7 1 3	1.5808	5	2 2 -1	1.5738	8	1 2 4	1.5796	19	3 3 4

were found to be almost identical with those reported by other authors.^{14,15,19–22}

Table 4 contains the crystallographic parameters of the vanadium(IV) oxo selenites obtained by the hydrothermal synthesis.

Vanadyl(IV) selenites were studied with IR spectroscopy and the obtained absorption spectra are presented in Figure 2.

The interpretation of the characteristic absorption bands in the IR spectra of the vanadyl(V) selenites was consistent with that of other authors with regard to the investigated selenites.^{18,24–30} In the high-frequency region of IR spectra (3600–3200 cm⁻¹) some absorption bands were registered that could be attributed to stretching vibrations of O–H bonds in water molecules of the crystallization water.^{27,28,31} In the middle frequency region of IR spectra

Table 4. Crystallographic data for vanadyl(IV) selenites.

Parameter	[VO(SeO ₃)(H ₂ O) ₂] · 0.5H ₂ O	VOSeO ₃ · H ₂ O	VOSeO ₃	VOSe ₂ O ₅
Colour	light-green	blue-green	grass-green	dark green
Space group	<i>C</i> 2/ <i>c</i>	<i>P</i> -1	<i>P</i> 2 ₁ / <i>c</i>	<i>P</i> 4 <i>cc</i>
<i>a</i> , [Å]	18.7773	5.9411	4.0147	11.2422
<i>b</i> , [Å]	6.2801	6.1461	9.7784	–
<i>c</i> , [Å]	10.5771	6.4142	7.9908	7.8553
<i>α</i> , [°]	–	91.802	–	–
<i>β</i> , [°]	116.438	101.462	99.347	–
<i>γ</i> , [°]	–	116.861	–	–
<i>Z</i>	8	2	4	8
<i>V</i> , [Å ³]	1116.85	202.76	309.53	992.87
<i>d_R</i> , [g cm ⁻³]	2.840	3.469	4.159	4.077

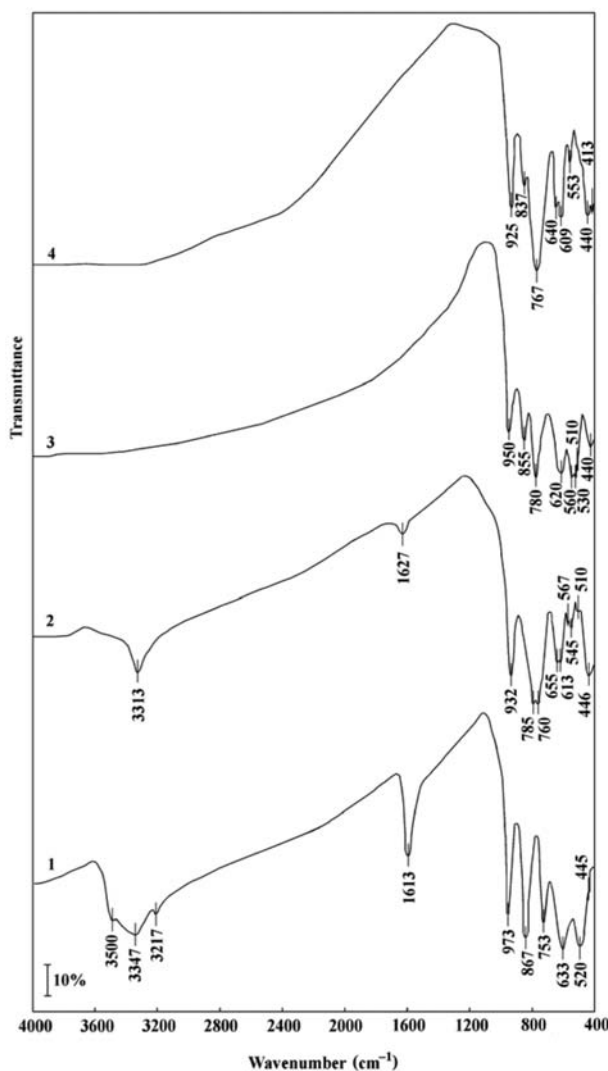
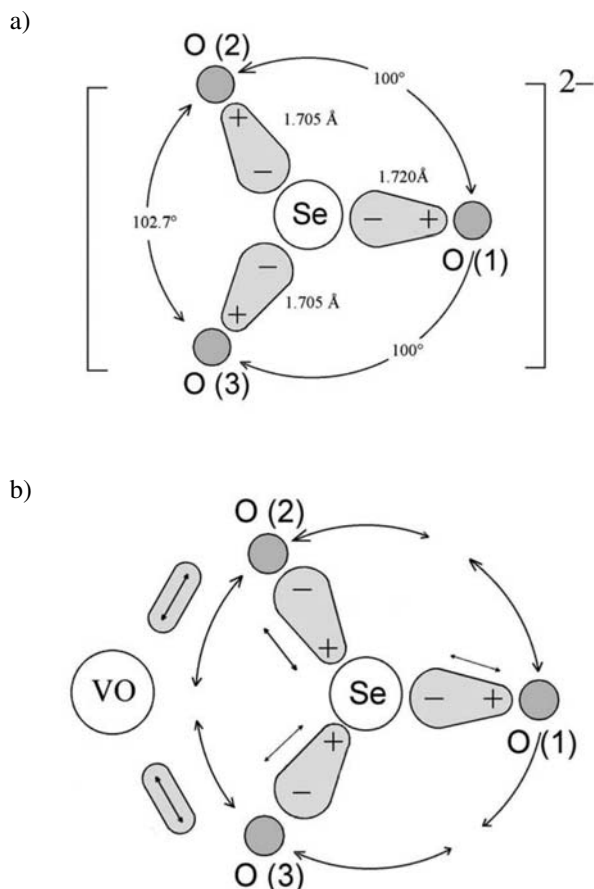


Figure 2. IR spectra of vanadium(IV) oxo selenites at 25 °C: 1 – $[\text{VO}(\text{SeO}_3)(\text{H}_2\text{O})_2] \cdot 0.5\text{H}_2\text{O}$, 2 – $\text{VOSeO}_3 \cdot \text{H}_2\text{O}$, 3 – VOSeO_3 , 4 – VOSe_2O_5 .

(1630 – 1610 cm^{-1}) other absorption bands were observed as a result of the bending vibrations of water molecules. The different location and the strength of water molecule bonds in the crystalline lattice of the selenites were the reason for the observed displacements of the vibration frequencies of the crystallohydrates. In the low frequency region (1000 – 400 cm^{-1}) a number of absorption bands were observed, as well as three types of characteristic bands attributed to $\nu(\text{V}=\text{O})$ in VO_3 group, $\nu(\text{V}-\text{O})$ in VO_3 group and $\nu(\text{Se}-\text{O})$ in SeO_3^{2-} ion, respectively. Such absorption bands were also reported by other authors.^{18,24,26–30}

Absorption bands characteristic for pure SeO_2 ,²² and SeO_3^{2-} ions were simultaneously observed in the spectrum of VOSe_2O_5 (Figure 2, spectrum 4).³² That could be explained with the structure and mechanism of the thermal decomposition of VOSe_2O_5 .^{21,22} The latter could be regarded as a product of a coordinate bonding of a molecule of



Scheme 1. A – SeO_3^{2-} anion and B – VOSeO_3 elementary crystal unit.

SeO_2 to VOSeO_3 . The bonds in the interval 950–860 cm^{-1} were due to $\nu_{\text{as}}(\text{SeO}_2)$; 840–810 cm^{-1} – $\nu_{\text{s}}(\text{SeO}_2)$; 790–750 cm^{-1} – $\nu_{\text{as}}(\text{Se}-\text{O})$; 700–600 cm^{-1} – $\nu_{\text{i}}(\text{Se}-\text{O})$; 600–550 cm^{-1} – $\nu_{\text{as}}(\text{Se}-\text{O}-\text{Se})$; 530–475 cm^{-1} – $\nu_{\text{s}}(\text{Se}-\text{O}-\text{Se})$; 480–380 cm^{-1} – $\delta(\text{SeO}_2)$, and the absorption band at 440 cm^{-1} resulted from $\delta(\text{V}-\text{O})$.^{18,23,26–30,32} All absorption bands observed in the IR-spectra of the obtained vanadyl(IV) selenites and their interpretations are summarized in Table 5.

On the basis of the IR spectra and literature data from quantum mechanical calculations, Scheme 1 was created, representing the SeO_3^{2-} anion and the perturbation of VO^{2+} cation in VOSeO_3 elementary crystal unit.

As can be seen from Scheme 1A the electron density of oxygen atoms in the selenite anion was pulled to the selenium atom compared to the isolated O^{2-} ion. Scheme 1B shows that, due to the effect of anion counterpolarization under the influence of the anion, the electron density of the bond O–Se was pulled towards the positive charge.³² Depending on cation nature and its polarizing ability, the degree of the counterpolarization was different which resulted in different vibration frequencies of the corresponding bonds. For instance, the shoulder at 785 cm^{-1} was due to the

Table 5. IR data (cm⁻¹) for different vanadyl(IV) selenites.

[VO(SeO ₃)(H ₂ O) ₂] · 0.5H ₂ O	VOSeO ₃ · H ₂ O	VOSeO ₃	VOSe ₂ O ₅	Band assignment
3500m				δ̄(HOH)(H ₂ O)
3347b				
3217m				
1613vs	1627m			ν(O–H)(H ₂ O)
973vs	932vs	950vs	925vs	v _s (V=O)(VO ₃)
				v _{as} (SeO ₂)
867vs		855s		v _{as} (V–O)(VO ₃)
			837m	v _s (SeO ₂)
	785s			v _{as} (Se–O)(SeO ₃ ²⁻)
753vs	760s	780vs	767vs	v _s (Se–O)(SeO ₃ ²⁻)
	655m		640m	δ(V ₂ O ₂)
633s	613m	620s		v _s (Se–O)(SeO ₃ ²⁻)
			609s	v _{as} (Se–O–Se)
			553s	δ̄(V–O–V)
	567w	560m		
	545m	530m		
	510sh	510sh		
520s				δ̄(SeO ₃)
445sh	446s	440m	440s	δ̄(V–O)(VO ₃)
			413m	δ̄(SeO ₂)

vs – very strong, s – strong, m – medium, w – weak, b – broad, sh – shoulder, ν – stretching, v_s – symmetric stretching, v_{as} – asymmetric stretching and δ – bending vibrations.

asymmetric stretching vibrations of the Se–O bond(1), while the high intensity band with absorption maximum at 446 cm⁻¹ was due to the superposition of symmetric and asymmetric stretching vibrations of the Se–O(2,3) bonds with respect to the deformation vibrations of the V–O bond.

The thermal stability of the initial reagent VOSO₄ · 2H₂O and the synthesized VOSeO₃ · H₂O were studied using non-isothermal thermogravimetry. Figure 3 presents the corresponding TG, DTG and DTA curves.

Three pronounced steps could be observed along the TG curve (curve 1), and three endo-effects along the DTA curve – at 150, 265 and 600 °C, respectively. The thermal decomposition of VOSO₄ · 2H₂O included three steps: the first – dehydration, the second and the third – decomposition to V₂O₅. A justification for such an assumption was found in the described mechanism of thermal decomposition of other sulfates.^{33,34}

During the thermal processing of VOSeO₃ · H₂O two steps were observed along the TG curve (curve 2), and two endo-effects along the DTA curve – at 140 and 490 °C, respectively. The first effect could be related with the separation of the crystallization water, and the second – with the decomposition of VOSeO₃ to V₂O₄, which was confirmed by the results from the chemical and X-ray diffraction analyses. Based on the method of Tang et al. for kinetics calculations of topochemical reactions under non-isothermal conditions of heating, the values of the activation energies of the decomposition processes for both compounds were calculated at each stage to be as follows: I stage of VOSO₄ · 2H₂O decomposition – 88.2 kJ mol⁻¹, II stage – 129.4 kJ mol⁻¹, III stage – 183.7 kJ mol⁻¹ and I

stage of VOSeO₃ · H₂O decomposition – 58.5 kJ mol⁻¹, II stage – 303.0 kJ mol⁻¹.³⁴

The results from the solubility isotherms, chemical, powder X-ray diffraction and thermal analyses, and IR spectroscopy, were summarized in Figure 4, where the solubility polytherm of the system VOSeO₃ – SeO₂ – H₂O is presented, as well as the crystallization fields of the corresponding vanadyl(IV) selenites.

As can be seen from Figure 4 four crystallization fields were formed at the applied temperatures within the investigated SeO₂ concentration interval. The compound [VO(SeO₃)(H₂O)₂] · 0.5 H₂O existed till 37 mass% SeO₂ and temperatures up to 230 °C. The crystallization field of VOSeO₃ · H₂O expanded between 16 mass% SeO₂ and temperature 300 °C and 70 mass% SeO₂ at temperatures below 160 °C. With the temperature increase to 220 °C a solid phase of VOSeO₃ was formed, which existed till 32 mass% SeO₂ and 300 °C. The crystallization field of VOSe₂O₅ was located in the temperature interval from 220 °C to 300 °C and above 32 mass% SeO₂.

With the increase of the temperature the water content decreased in the composition of the vanadyl(IV) selenites, while only at high temperatures the increase of the concentration of SeO₂ led to the formation of thermodynamically stable phases with higher content of SeO₂. At lower concentration of selenium dioxide (< 30 mass%) and temperature increase the stability of the phases could be sequenced as follows: [VO(SeO₃)(H₂O)₂] · 0.5 H₂O → VOSeO₃ · H₂O → VOSeO₃, while at higher concentrations of SeO₂ (>40 mass%) the following transition was observed: VOSeO₃ · H₂O → VOSeO₃ → VOSe₂O₅. At

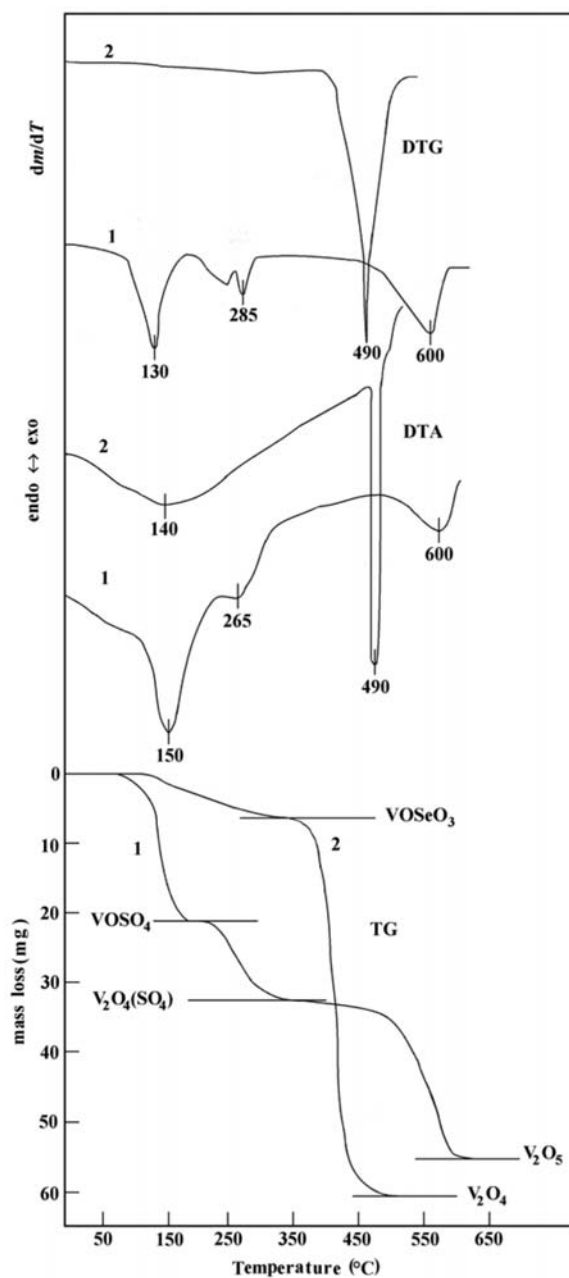


Figure 3. TG, DTA, DTG curves of decomposition of: 1– $\text{VOSO}_4 \cdot 2\text{H}_2\text{O}$ and 2 – $\text{VSeO}_3 \cdot \text{H}_2\text{O}$

constant temperature, the decrease of the SeO_2 concentration led to an equilibrium shift towards selenites with lower content of selenium dioxide in their composition. In this case the hydrolysis was relieved, as well as the formation of higher crystal hydrates.

4. Conclusions

All the data acquired from the chemical, X-ray diffraction and thermal analyses and IR spectroscopy in co-

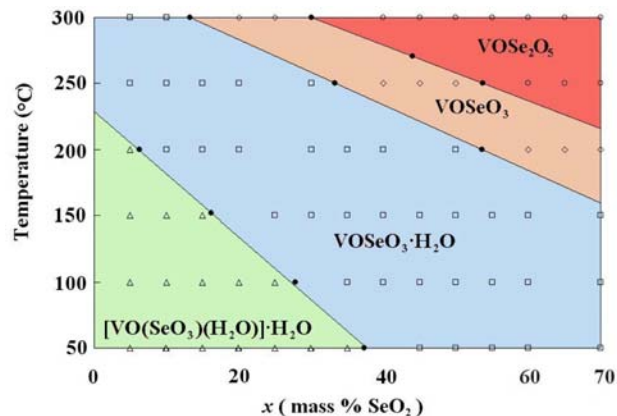


Figure 4. Crystalization fields of selenites in $\text{VSeO}_3 - \text{SeO}_2 - \text{H}_2\text{O}$ system.

njunction with the *Schreinemaker's* method were used for the plotting of solubility isotherms of the system $\text{VSeO}_3 - \text{SeO}_2 - \text{H}_2\text{O}$ within broad temperature and concentration intervals, as well as for the plotting of the crystallization fields of the different vanadyl(IV) selenites. In the present paper for the first time the absorption bands in the region $4000\text{--}400\text{ cm}^{-1}$ were given for all studied vanadyl(IV) selenites. The obtained data could be useful for synthesis of these pure compounds. The results, concerning the thermal stability of VSeO_3 are very important, because by its pretreatment in reduction medium very pure vanadyl selenide may be obtained.

5. References

1. T. Ozeki, H. Ichida, Yu. Sasaki, *Acta Cryst.* **1987**, C 43, 1662–1665.
2. Y. Oka, T. Yao, N. Yamamoto, *J. Solid. State Chem.* **2000**, 152, 486–491.
3. R. Shpanchenko, V. V. Chernaya, E. Antipov, J. Haderman, E. E. Kaul, C. Geibel, *J. Solid. State Chem.* **2003**, 173, 244–250.
4. A. Mitiaev, A. Mironov, R. Shpanchenko, E. Antipov, *Acta Cryst.* **2004**, C 60, i56–i58.
5. H. Jiang, F. Kong, Y. Fan, J. Mao, *Inorg. Chem.* **2008**, 47, 7430–7437.
6. S. H. Kim, J. Yeon, A. S. Sefat, D. G. Mandrus, P. Sh. Halasyamani, *Chem. Mater.* **2010**, 22, 6665–6672.
7. Zh. Shi, D. Zhang, Zh. Feng, G. Li, Zh. Dai, W. Fu, X. Chen, J. Hua, *J. Chem. Soc. Dalton Trans.* **2002**, 9, 1873–1874.
8. Zh. Dai, G. Li, Zh. Shi, W. Fu, W. Dong, J. Xu, Sh. Feng, *Solid State Sciences* **2004**, 6, 91–96.
9. D. Xiao, H. An, E. Wang, Ch. Sun, L. Xu, *J. Coord. Chem.* **2006**, 59, 827–835.
10. Zh. Lian, J. Zhang, Y. Gu, T. Wang, T. Lou, *J. Mol. Struct.* **2009**, 919, 122–127.
11. K. Srivastava, *Molecular and Cellular Biochemistry* **2000**, 206, 177–182.

12. M. Evangelou, *Critical Reviews in Oncology/Hematology* **2002**, 42, 249–265.
13. J.-C. Trombe, R. Enjalbert, A. Gleizes, J. Galy, J.-P. Renard, Y. Journaux, M. Verdaguer, *New J. Chem.* **1987**, 11, 321–328.
14. S.-H. Kim, P. Sh. Halasyamani, B. C. Melot, R. Seshadri, M. A. Green, A. S. Sefat, D. Mandrus, *Chem. Mater.* **2010**, 22, 5074–5083.
15. W. T. A. Harrison, *Acta Cryst.* **2010**, C 66, i61–i63.
16. M. Launay, F. Boucher, P. Gressier, G. Ouvrard, *J. Solid State Chem.* **2003**, 176, 556–566.
17. Y. H. Kim, K.-S. Lee, Y.-U. Know, O. H. Han, *Inorg. Chem.* **1996**, 35, 7394–7398.
18. R. Rocha, E. Baran, *Z. anorg. allg. Chem.* **1988**, 564, 141–147.
19. W. T. A. Harrison, *Acta Cryst.* **2010**, C 66, i61–i63.
20. G. Huan, J. W. Johnson, A. J. Jacobson, D. P. Goshorn, J. S. Merola, *Chem. Mater.* **1991**, 3, 539–541.
21. J.-C. Trombe, R. Enjalbert, A. Gleizes, J. Galy, *C. R. Acad. Sc. Paris, Serie-II* **1983**, 297, 667–670.
22. G. Meunier, M. Bertaud, J. Galy, *Acta Cryst.* **1974**, B 30, 2834–2839.
23. P. Millet, R. Enjalbert, J. Galy, *J. Solid State Chem.* **1999**, 147, 296–303.
24. W. T. A. Harrison, J. T. Vaughey, A. J. Jacobson, D. P. Goshorn, J. W. Johnson, *J. Solid State Chem.* **1995**, 116, 77–86.
25. L. Vlaev, V. Georgieva, E. Popova, *Bulg. Chem. Ind.* **2004**, 75, 28–31.
26. V. P. Verma, *Thermochim. Acta* **1999**, 327, 63–102.
27. L. T. Vlaev, S. D. Genieva, G. G. Gospodinov, *J. Thermal Anal. Cal.* **2005**, 81, 469–475.
28. L. T. Vlaev, S. D. Genieva, V. G. Georgieva, *J. Thermal Anal. Cal.* **2006**, 86, 449–456.
29. L. T. Vlaev, M. P. Tavlieva, *J. Thermal Anal. Cal.* **2007**, 90, 385–392.
30. A. A. Arndt, M. S. Wickleder, *Eur. J. Inorg. Chem.* **2007**, 2007, 4335–4339.
31. R. L. Frost, E. C. Keeffe, *J. Raman Spectrosc.* **2008**, 39, 1789–1793.
32. V. P. Verma, A. Khushu, *J. Thermal Anal.* **1989**, 35, 1157–1163.
33. P. Masset, J. Y. Poinso, J. C. Poignet, *J. Therm. Anal. Cal.* **2006**, 83, 457–462.
34. L. Vlaev, V. Georgieva, *J. Thermal Anal. Cal.* **2007**, 88, 805–812.

Povzetek

Raziskali smo topnost sistema $\text{VOSeO}_3\text{-SeO}_2\text{-H}_2\text{O}$ v temperaturnem območju 50–300 °C. Narisali smo fazni diagram vanadil(IV) selenitov in za različne faze določili polja kristalizacije. V odvisnosti od pogojev hidrotermalne sinteze smo izolirali nekaj tipov selenitov – $[\text{VO}(\text{SeO}_3)(\text{H}_2\text{O})_2] \cdot 0.5 \text{H}_2\text{O}$, $\text{VOSeO}_3 \cdot \text{H}_2\text{O}$, VOSeO_3 in VOSe_2O_3 , ki smo jih okarakterizirali s kemijsko, termično in rentgensko praškovno analizo ter IR spektroskopijo.